Mesenchymal cells reactivate Snail1 expression to drive three-dimensional invasion programs

R. Grant Rowe,[1,6] Xiao-Yan Li,[1,2] Yuexian Hu,[1,2] Thomas L. Saunders,[1,3] Ismo Virtanen,[7] Antonio Garcia de Herreros,[8] Karl-Friedrich Becker,[9] Signe Ingvarsen,[10] Lars H. Engelholm,[10] Guido T. Bommer,[1] Eric R. Fearon,[1,4,5] and Stephen J. Weiss[1,2]

[1]Division of Molecular Medicine and Genetics, Department of Internal Medicine, [2]the Life Sciences Institute, [3]the Biomedical Research Core Facilities, [4]Department of Human Genetics, [5]Department of Pathology, and [6]Program in Cell and Molecular Biology, University of Michigan, Ann Arbor, MI 48109
[7]Institute of Biomedicine/Anatomy, University of Helsinki, FIN-00014 Helsinki, Finland
[8]Programa de Recerca en Cancer, Institut Municipal d'Investigació Mèdica Hospital del Mar Universitat Pompeu Fabra, 08003 Barcelona, Spain
[9]Institute of Pathology, Technical University of Munich, D-81675 Munich, Germany
[10]The Finsen Laboratory, Department 3735, Rigshospitalet, DK-2200 Copenhagen N, Denmark

Epithelial–mesenchymal transition (EMT) is required for mesodermal differentiation during development. The zinc-finger transcription factor, Snail1, can trigger EMT and is sufficient to transcriptionally reprogram epithelial cells toward a mesenchymal phenotype during neoplasia and fibrosis. Whether Snail1 also regulates the behavior of terminally differentiated mesenchymal cells remains unexplored. Using a *Snai1* conditional knockout model, we now identify Snail1 as a regulator of normal mesenchymal cell function. Snail1 expression in normal fibroblasts can be induced by agonists known to promote proliferation and invasion in vivo. When challenged within a tissue-like, three-dimensional extracellular matrix, Snail1-deficient fibroblasts exhibit global alterations in gene expression, which include defects in membrane type-1 matrix metalloproteinase (MT1-MMP)-dependent invasive activity. Snail1-deficient fibroblasts explanted atop the live chick chorioallantoic membrane lack tissue-invasive potential and fail to induce angiogenesis. These findings establish key functions for the EMT regulator Snail1 after terminal differentiation of mesenchymal cells.

Introduction

Snail1, a zinc finger–type transcriptional repressor, initiates an epithelial–mesenchymal transition (EMT) that is critical for the morphogenetic events that characterize developmental programs such as gastrulation (Carver et al., 2001; Nieto, 2002; Murray et al., 2007). Snail1 triggers this transdifferentiation program, in part, by repressing epithelial markers and related cell–cell junction proteins while coordinately acting as a major cytoskeletal regulator (Batlle et al., 2000; Cano et al., 2000; Moreno-Bueno et al., 2006; Peinado et al., 2007). The aberrant postnatal expression of Snail1 is sufficient to confer a mesenchymal, fibroblast-like phenotype in differentiated epithelial cells during pathological states associated with cancer and fibrosis (Yook et al., 2005, 2006; Boutet et al., 2006; Moreno-Bueno et al., 2006; Olmeda et al., 2007a,b; Peinado et al., 2007).

At sites of active tissue remodeling, changes in vascular permeability disperse serum-derived soluble growth factors within the interstitial compartment, which serve to activate signal transduction cascades in resident fibroblasts (Martin, 1997; Bhowmick et al., 2004; Dong et al., 2004; Orimo et al., 2005; Klapholz-Brown et al., 2007). Accordingly, these agonists trigger changes in gene expression programs that shift the fibroblast phenotype from a quiescent status to an "activated" state characterized by increased proliferation, tissue-invasive activity, and the induction of angiogenesis (Martin, 1997; Iyer et al., 1999; Bhowmick et al., 2004; Sabeh et al., 2004; Klapholz-Brown et al., 2007). Growth factors capable of promoting the activated fibroblast phenotype, such as PDGF-BB, have been identified (Dong et al., 2004; Gao et al., 2005), but key transcription factors that regulate downstream gene programs

Correspondence to Stephen J. Weiss: sjweiss@umich.edu

Abbreviations used in this paper: adeno-Cre, adenoviral Cre recombinase; β-gal, β-galactosidase; CAM, chorioallantoic membrane; EMT, epithelial–mesenchymal transition; MT1-MMP, membrane type-1 matrix metalloproteinase; GO, gene ontology.

© 2009 Rowe et al. This article is distributed under the terms of an Attribution–Noncommercial–Share Alike–No Mirror Sites license for the first six months after the publication date (see http://www.jcb.org/misc/terms.shtml). After six months it is available under a Creative Commons License (Attribution–Noncommercial–Share Alike 3.0 Unported license, as described at http://creativecommons.org/licenses/by-nc-sa/3.0/).

The Rockefeller University Press $30.00
J. Cell Biol. Vol. 184 No. 3 399–408
www.jcb.org/cgi/doi/10.1083/jcb.200810113

remain largely uncharacterized. Herein, we identify Snail1 as a critical regulator of both fibroblast gene expression programs and fibroblast function in vitro as well as in vivo. The results demonstrate that Snail1, a master EMT inducer, continues to subserve vital cellular functions following mesenchymal cell terminal differentiation.

Results and discussion

Under serum-free conditions, fibroblasts do not express detectable levels of Snail1 mRNA or protein (Fig. 1, A and B). In contrast, in the presence of 10% serum or PDGF-BB, both Snail1 mRNA and intranuclear protein levels are strongly induced in mouse as well as human fibroblasts (Fig. 1, A–C). In epithelial cells, Snail1 protein half-life is controlled by GSK3-β–dependent and –independent ubiquitination pathways that lead to proteasome-mediated Snail1 destruction (Zhou et al., 2004; Yook et al., 2005, 2006; Vernon and LaBonne, 2006). As expected, blockade of fibroblast proteasome activity with the inhibitor, MG132, results in a marked accumulation of the Snail1 protein (Fig. 1 B). In the GSK3-β–dependent pathway, Snail1 is marked for ubiquitination after phosphorylation of its N-terminal domain (Zhou et al., 2004; Vernon and LaBonne, 2006; Yook et al., 2006). As PDGF-BB signaling can inhibit GSK3-β activity via the phosphatidylinositol 3-kinase (PI3K)/Akt-dependent phosphorylation of GSK3-β serine 9 (Ser^9; Julien et al., 2007), Akt phosphorylation, Ser^9 phosphorylation, and Snail1 protein levels were monitored in fibroblasts in the absence or presence of the PI3K inhibitor, LY 294002. As predicted, treatment of serum-starved fibroblasts with PDGF-BB induces an increase in phospho-Akt and Ser^9 GSK3-β levels in tandem with an increase in Snail1 protein (Fig. 1, D and E). In the presence of LY 294002, however, both Akt and Ser^9 GSK3-β phosphorylation are blocked, and Snail1 levels fall to undetectable levels (Fig. 1, D and E).

Snai1-deficient mice die early in development before the differentiation of mesodermal lineages (Carver et al., 2001; Peinado et al., 2007). Hence, we generated mice in which *Snai1* could be inactivated in selected tissues by Cre/loxp-mediated recombination (Fig. 2, A–C). Fibroblasts isolated from a $Snai1^{+/fl}$ mouse were treated with an adenoviral Cre recombinase construct (adeno-Cre) or a control adenovirus (β-galactosidase [β-gal]), and recombination at the *Snai1* locus was verified by PCR. As shown in Fig. 2 D, although adeno–β-gal–infected fibroblasts yield P1/P2 amplicons corresponding to both the wild-type and loxp alleles of *Snai1*, adeno-Cre–infected fibroblasts yielded a single amplicon corresponding to the wild-type *Snai1* allele with P1 and P2, as well as a P3/P4 amplicon representing the $Snai1^-$ allele. Fibroblasts isolated from $Snai1^{fl/fl}$ mice and infected with adeno-Cre display a 95%

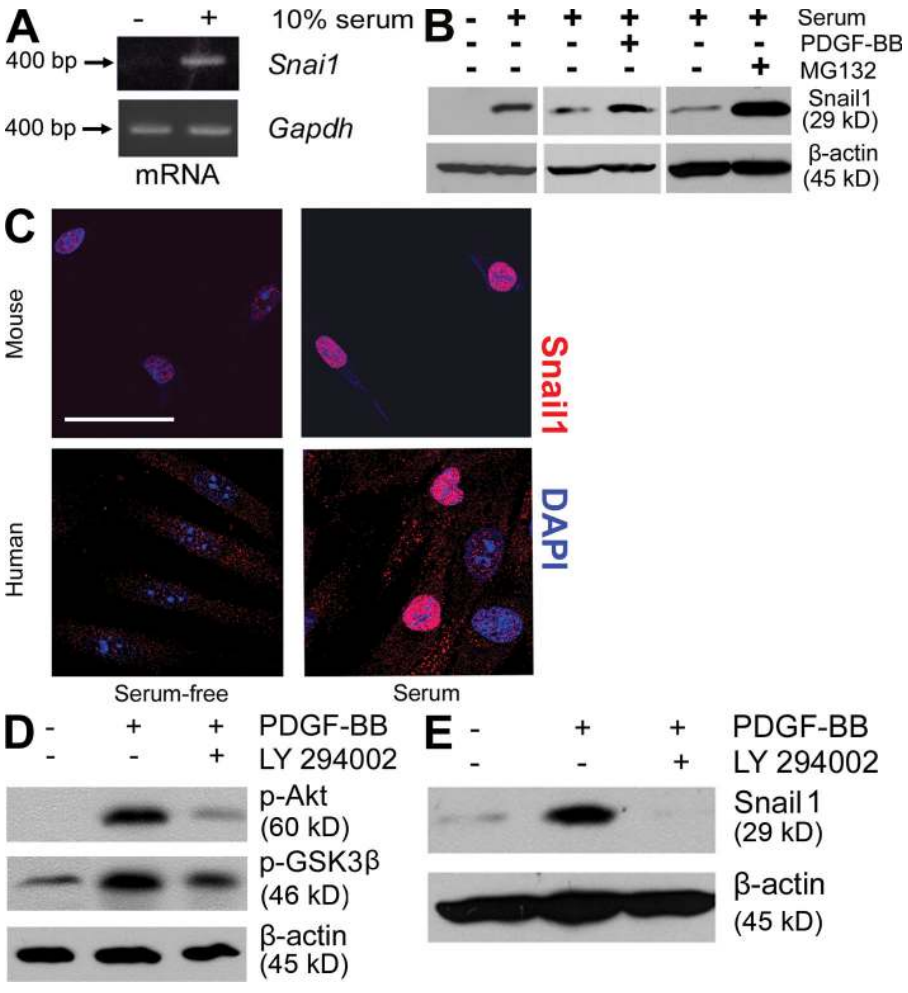

Figure 1. **Expression and regulation of Snail1 in activated fibroblasts.** (A) Mouse dermal fibroblasts were cultured in the presence or absence of 10% serum for 24 h, and Snail1 mRNA was assessed by RT-PCR. (B) Mouse dermal fibroblasts were cultured serum-free, or in the presence of 10% serum, serum plus 10 ng/ml PDGF-BB, or serum plus 10 μM MG132 for 24 h, and Snail1 protein was monitored by Western blotting. (C) Mouse fibroblasts (top) or human foreskin fibroblasts (bottom) were cultured serum-free or in the presence of 10% serum for 24 h, and Snail1 protein were localized by immunocytochemistry with the anti-Snail1 173EC2 monoclonal antibody (mouse fibroblasts) or the Sn9H2 monoclonal antibody (human fibroblasts). Nuclei were stained with DAPI (blue). Bar, 50 μm. (D) Mouse dermal fibroblasts were cultured serum-free for 48 h, followed by stimulation with 10 ng/ml PDGF-BB in the presence or absence of 10 μM LY294002 for 10 min. Levels of phospho-Ser^{473} Akt, phospho-Ser^9 GSK3-β, and β-actin were assessed by Western blotting. (E) Mouse dermal fibroblasts were cultured serum-free for 24 h, followed by stimulation with 10 ng/ml PDGF-BB for 12 h in the presence or absence of LY294002, and Snail1 protein levels were determined by Western blotting.

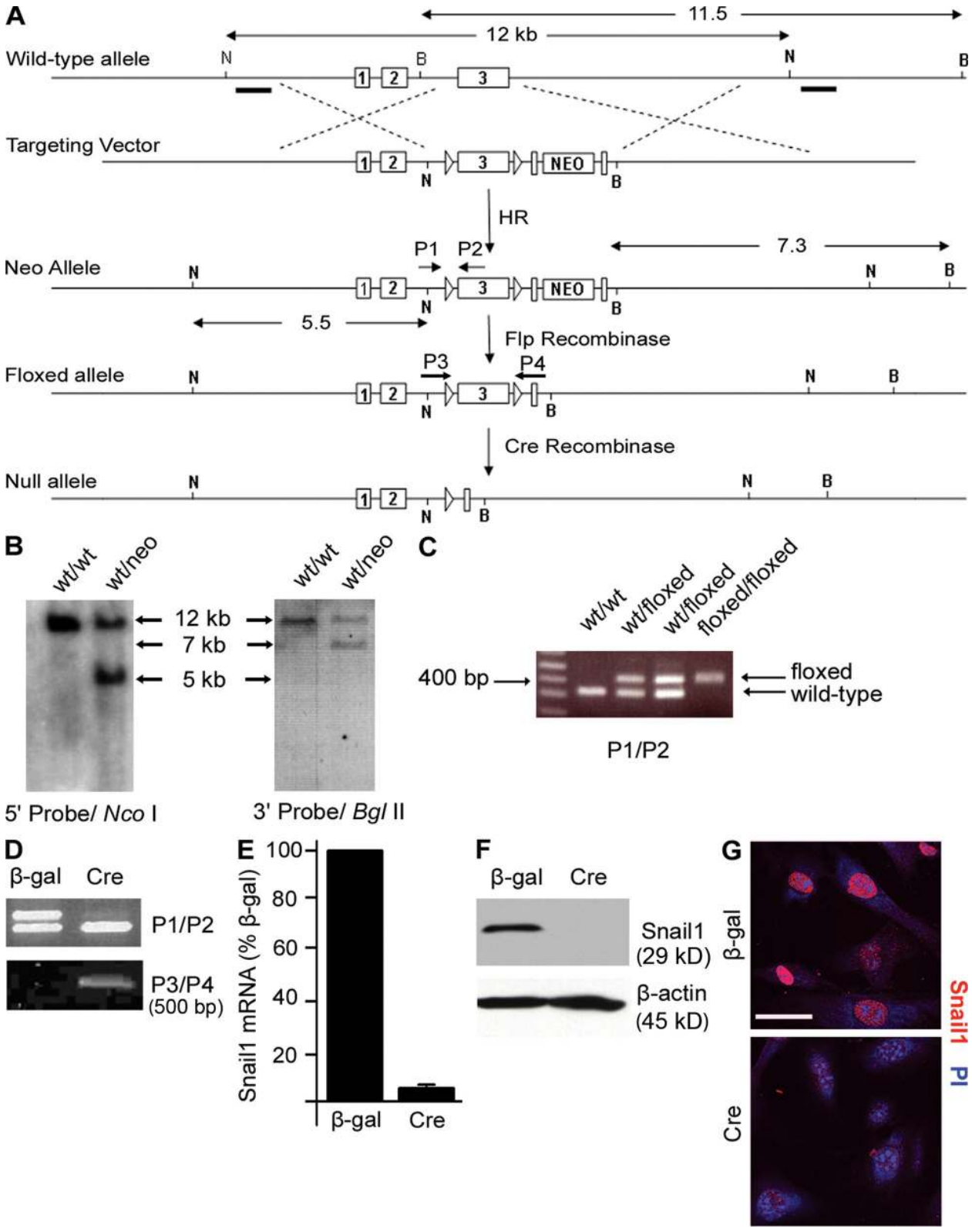

Figure 2. **A model of Snail1 deficiency in mouse fibroblasts.** (A) Schematic of targeting strategy used to generate a mouse *Snai1* conditional knockout allele. B, BglII; H, NcoI. (B) Embryonic stem cell clones were screened for recombination of the targeting vector at the 5′ (NcoI) or 3′ (BglII) ends. (C) Example of genotyping results demonstrating amplification of the $Snai1^{wt}$ and $Snai1^{fl}$ alleles with P1 and P2. (D) $Snai1^{wt/fl}$ dermal fibroblasts were infected either with a control adenovirus (β-gal) or adeno-Cre, and recombination of the $Snai1^{fl}$ allele was assessed by the loss of the 420–base pair amplicon when genomic DNA was amplified with P1 and P2 (top) and the appearance of a single amplicon with P3 and P4 (bottom). (E–G) $Snai1^{fl/fl}$ dermal fibroblasts were infected with either a control adenovirus or a Cre adenovirus, and *Snai1* recombination was assessed by quantitative PCR (E), Western blotting (F), or immunocytochemistry for Snail1 with mAb 173EC2 (red) with propidium iodide (PI) counterstaining (blue; G). Error bars indicate ± 1 SEM. Bar, 30 μm.

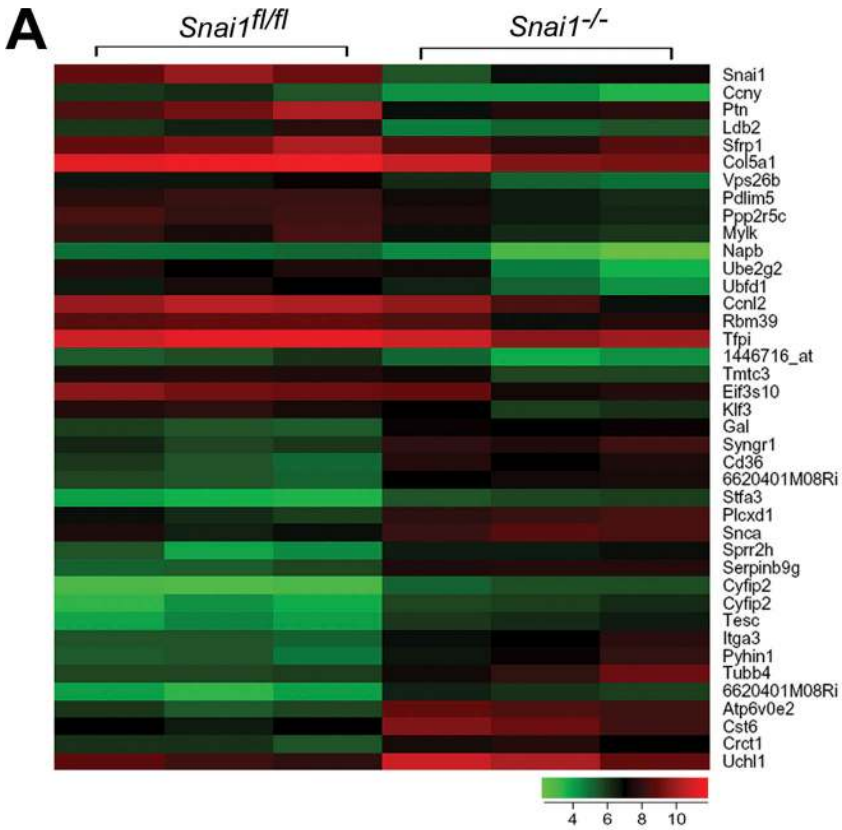

C

Gene Symbol	Gene Name	p-value	Fold-change
Cttn	cortactin	0.003	-1.74
Enah	enabled homolog	0	-2.27
Ezr	ezrin	0	2.6
Msn	moesin	0.001	-2
Rhoa	Ras homolog gene family, member A	0	-1.99
Rock1	Rho-associated coiled-coil containing protein kinase 1	0.004	-1.71
Mylk	myosin, light polypeptide kinase	0	-2.3
Tpm1	tropomyosin 1, alpha	0	-2.08
Mmp14	matrix metallopeptidase 14 (membrane-inserted)	0.003	-1.88

Figure 3. **Snail1 is a master regulator of fibroblast gene expression programs.** (A) Heat map of microarray data for three biological replicates of Snail1$^{fl/fl}$ and Snail1$^{-/-}$ fibroblasts. The 20 most highly up-regulated and down-regulated transcripts in Snail1$^{-/-}$ fibroblasts are presented. The key on the bottom assigns heat map colors to the absolute gene expression value on a log2 scale. (B) GO terms identifying biological processes differentially expressed in *Snai1*$^{fl/fl}$ and deficient fibroblasts. (C) List of motility- and invasion-associated genes regulated by Snail1 in fibroblasts.

reduction in Snail1 mRNA, whereas Snail1 protein expression is undetectable by Western blotting or immunocytochemistry (Fig. 2, F and G).

In addition to its well-defined role in promoting EMT, Snail1 can regulate cell cycle progression and sensitivity to proapoptotic stresses (Vega et al., 2004; Barrallo-Gimeno and Nieto, 2005; Escriva et al., 2008). Snail1-deficient fibroblasts proliferate, however, at normal rates, with no observed changes in apoptosis under serum-free conditions (Fig. S1, A and B, available at http://www.jcb.org/cgi/content/full/jcb.200810113/DC1).

Furthermore, though Snail1 can promote a motile phenotype in epithelial cells (Barrallo-Gimeno and Nieto, 2005; Peinado et al., 2007), Snail1-deleted fibroblasts migrate at rates comparable to wild-type fibroblasts in a two-dimensional wound assay (Fig. S1, C and D). Likewise, whereas increased fibronectin synthesis and matrix assembly are characteristic features of EMT programs (Barrallo-Gimeno and Nieto, 2005; Peinado et al., 2007), Snail1-deficient fibroblasts deposit a fibronectin matrix at rates comparable to control fibroblasts (Fig. S1 E). Consequently, insights into Snail1 function were alternatively sought by interrogating the gene expression patterns of Snail1-deleted fibroblasts. Recent studies have demonstrated that cell behavior in vitro more closely recapitulates that observed in vivo when cells are cultured within a 3D ECM (Hotary et al., 2003; Yamada and Cukierman, 2007; Zhou et al., 2008). Hence, Snail1 wild-type and deficient cells were suspended in type I collagen matrices, the dominant matrix component of interstitial tissues (Grinnell, 2003; Sabeh et al., 2004), and subjected to transcriptional profiling. Using cutoffs of $P \leq 0.005$ and a minimum fold change of 1.5, Snail1 deficiency in fibroblasts exerts a global effect on transcription, with >1,000 significant changes in gene expression detected (Fig. 3 A and Table S1, available at http://www.jcb.org/cgi/content/full/jcb.200810113/DC1). Gene ontology (GO) analysis further demonstrates that Snail1 governs multiple processes critical to fibroblast motile behavior, including adhesion, migration, and proteolysis (Fig. 3 B). Snail1 deletion did not trigger a mesenchymal-to-epithelial transdifferentiation process, as assessed by transcriptional analysis, which suggests that Snail1 is required for the induction, but not maintenance, of the mesenchymal phenotype during development.

To assess the consequences of Snail1 loss on 3D ECM invasion, a critical component of fibroblast wound and tumor responses (Martin, 1997; Grinnell, 2003; Bhowmick et al., 2004; Sabeh et al., 2004; Orimo et al., 2005), cells were embedded within a 3D bed of type I collagen. Snail1-deleted, but not Snail1-rescued, fibroblasts displayed a significant defect in their ability to negotiate the type I collagen barrier (Fig. 4, A and B; and Fig. S2, A and B, available at http://www.jcb.org/cgi/content/full/jcb.200810113/DC1). Focusing on candidate genes implicated previously in 3D cell motility and invasion (Yamaguchi and Condeelis, 2007; Olson and Sahai, 2008; Sakurai-Yageta et al., 2008), probe sets corresponding to transcripts for cortactin (*Cttn*), enabled homologue (*Enah*), ezrin, moesin, rhoA, ROCK1, myosin light chain kinase, tropomyosin, and membrane type-1 matrix metalloproteinase (MT1-MMP; *Mmp14*) are significantly altered in Snail1-deficient fibroblasts (Fig. 3 C). Consistent with the altered patterns of gene expression revealed by the microarray data and confirmed by quantitative PCR (Fig. S2C), Snail1-deficient fibroblasts exhibit a significant reduction in the cortactin-rich membrane protrusions that mark invadopodia, the actin-rich, cellular processes that focus proteolytic activity at sites of cell–ECM contact (i.e., 83.3 ± 8.3% cortactin-positive processes in wild-type fibroblasts vs. 31.2 ± 13.2% in Snail1-deleted fibroblasts; $P < 0.01$; Fig. 4 C; Gimona et al., 2008).

As cortactin-rich invadopodia play a critical role in recruiting MT1-MMP, a membrane-anchored collagenase critical for cell invasion, to zones of pericellular proteolysis (Artym et al., 2006; Clark et al., 2007; Li et al., 2008), wild-type and Snail1-deficient fibroblasts were cultured with fibrillar gels of Alexa 594–labeled type I collagen, and collagenolysis was monitored (Sabeh et al., 2004). Whereas wild-type fibroblasts generate collagenolytic zones that are associated with adhesive sites enriched for actin spikes and cortactin, Snail1-deficient fibroblasts exhibit a significantly diminished ability to degrade collagen or mobilize invadopodia-like structures (Fig. 4, D and E). In accordance with these collagenolytic defects, invadopodial clusters of MT1-MMP and cortactin localized at the fibroblast–collagen interface are reduced by ∼80% in Snail1-deficient cells (Fig. 4, F and G). Reconstitution of Snail1-deficient fibroblasts with full-length human Snail1 normalizes expression of cortactin and MT1-MMP (Fig. S2 D). Furthermore, consistent with GO enrichment scores that did not detect changes in cell cycle or apoptosis regulation, wild-type or Snail1-deleted fibroblasts embedded within 3D collagen gels proliferate at indistinguishable rates (7.8 ± 3.2% Ki67-positive for Snail1 wild-type cells vs. 8.1 ± 1.4% Ki67-positive for Snail1-null cells; $n = 3$) and display similar low levels of apoptosis (Snail1 wild-type, 1.6 ± 0.8%; Snail1-null, 1.4 ± 1.4%; assessed by TUNEL; $n = 3$).

Though Snail1-deficient cells display defects in the pericellular proteolysis and invasion of homogeneous collagenous barriers in vitro, connective tissue barriers in vivo are more complex, multimolecular composites of ECM macromolecules (Grinnell, 2003; Hotary et al., 2003; Yamada and Cukierman, 2007; Zhou et al., 2008). As such, wild-type and Snail1-deleted fibroblasts were cultured atop the chorioallantoic membrane (CAM) of live chick embryos (Sabeh et al., 2004), a tissue characterized by a type IV collagen-rich basement membrane and an underlying interstitium containing both type I and type III collagens (the stroma also contains blood vessels circumscribed by type IV collagen-positive basement membranes; Fig. 5 A). Although wild-type fibroblasts efficiently breach the CAM basement membrane and invade into the underlying stroma, Snail1-deficient fibroblasts exhibit a complete defect in invasion and fail to penetrate the CAM surface (Fig. 5, B and C), a phenotype identical to that described previously for MT1-MMP–null fibroblasts (Sabeh et al., 2004). In vivo, fibroblasts can initiate neovascularization during wound healing (Martin, 1997), but Snail1-deficient fibroblasts also demonstrate a significantly attenuated ability to induce neovessel formation (Fig. 5, B and D). Neither proliferative nor apoptotic indices of the fibroblasts are affected in the CAM model (Fig. 5, E and F). Collectively, the data identify Snail1 as a master regulator of activated fibroblast function in vivo by controlling tissue-invasive as well as proangiogenic functions.

Snail1 exerts global effects on epithelial cell gene expression by binding consensus sequences within the promoter regions of target genes while recruiting histone deacetylases, arginine methyltransferase, and DNA methyltransferases to chromatin remodeling complexes (Peinado et al., 2007; Herranz et al., 2008; Hou et al., 2008). Despite the remarkable range of Snail1's impact on epithelial cell fate determination, a functional role for Snail1 in terminally differentiated mesenchymal cells has not been explored previously. Unexpectedly, under 3D culture

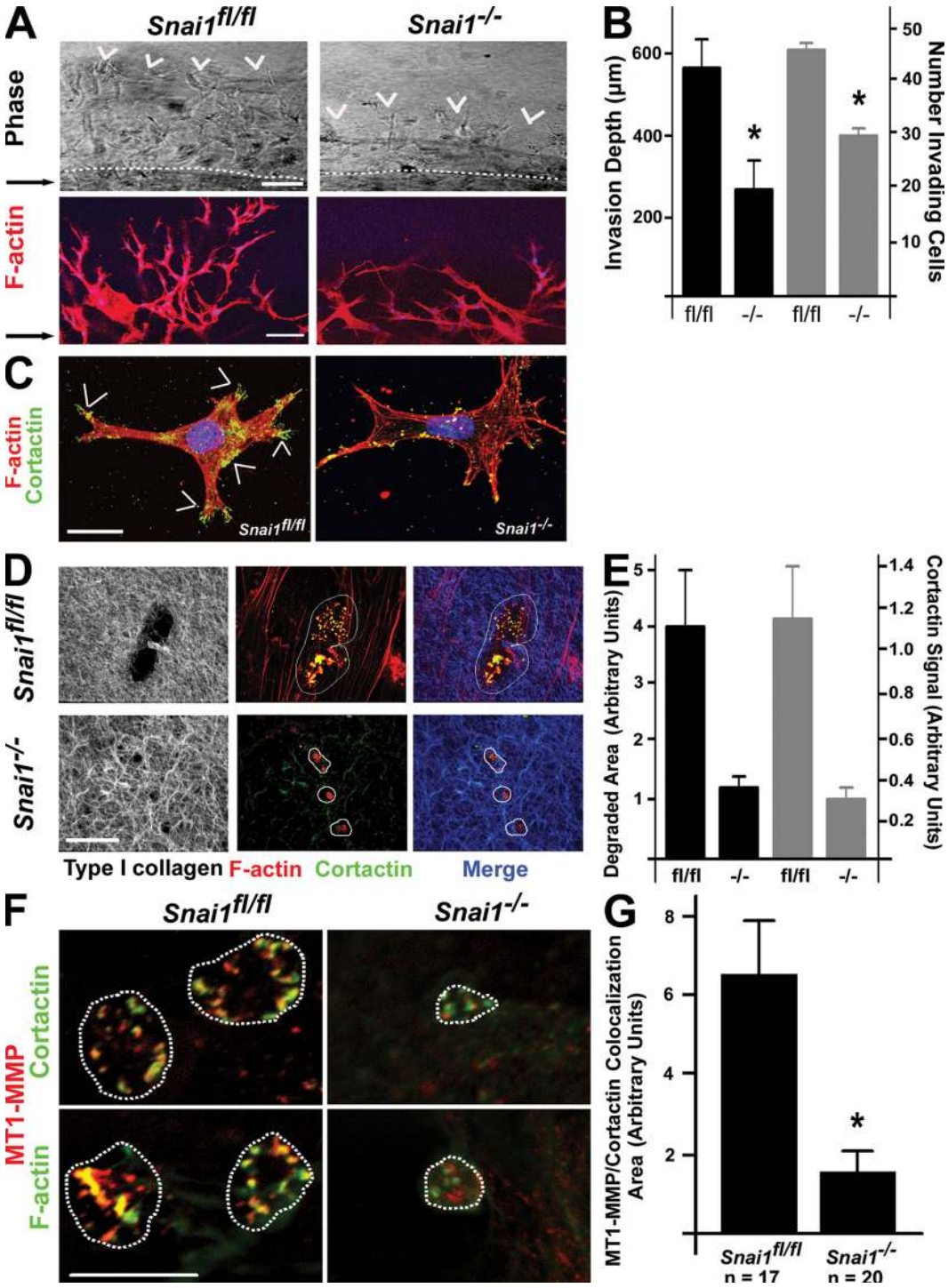

Figure 4. **Snail1 regulates the type I collagenolytic and 3D invasive activities of fibroblasts.** (A and B) *Snai1*$^{fl/fl}$ or *Snai1*$^{-/-}$ fibroblasts were embedded in a 100-µl plug of cross-linked, fibrillar type I collagen (2.2 mg/ml), which was embedded within a larger, cell-free collagen matrix in the presence of 10 ng/ml PDGF-BB and 10% serum. Migration was monitored over a 6-d culture period by phase-contrast microscopy, with arrowheads marking the advance of the invading front and the dotted line indicating the boundary between the inner and outer collagen gels (top) or after phalloidin staining in the bottom panels (red). (B) 3D invasion depth and the number of invading cells were measured after a 6-d culture period (n = 3; mean ± SEM). *, P < 0.01. (C) Snail1$^{fl/fl}$ or Snail1$^{-/-}$ fibroblasts were cultured in 3D collagen for 48 h and stained for cortactin (green), F-actin (red), and nuclei (DAPI, blue), and images were captured by confocal laser microscopy. Cortactin-rich cellular processes are indicated by arrowheads. (D and E) Fibroblasts were cultured atop a 3D bed of Alexa 594–labeled type I collagen (left, gray; right, blue) for 5 d, collagen degradation was monitored by confocal laser microscopy in sections costained for cortactin (green) and F-actin (D, middle and right panels, red), and photomicrographs were quantified using ImageQuant software. Degraded areas in left panels are demarcated by broken lines in the middle and right panels. (E) The degraded area and relative cortactin signal are presented as representative results of three experiments with the mean ± SEM (*, P < 0.05). (F and G) Snail1$^{fl/fl}$ or Snail1$^{-/-}$ fibroblasts were cultured on a bed of type I collagen and costained for MT1-MMP (red) and either cortactin (top, green) or F-actin (bottom, green; 60× magnification). The broken lines in F demarcate the invadopodial clusters used for colocalization analysis. (G) MT1-MMP signal colocalizing with cortactin and actin within invadopodia clusters was quantified using MetaMorph software. *, P < 0.005. Error bars indicate ± 1 SEM. Bars: (A, top) 200 µm; (A, bottom) 100 µm; (C and D) 10 µm; (F) 5 µm.

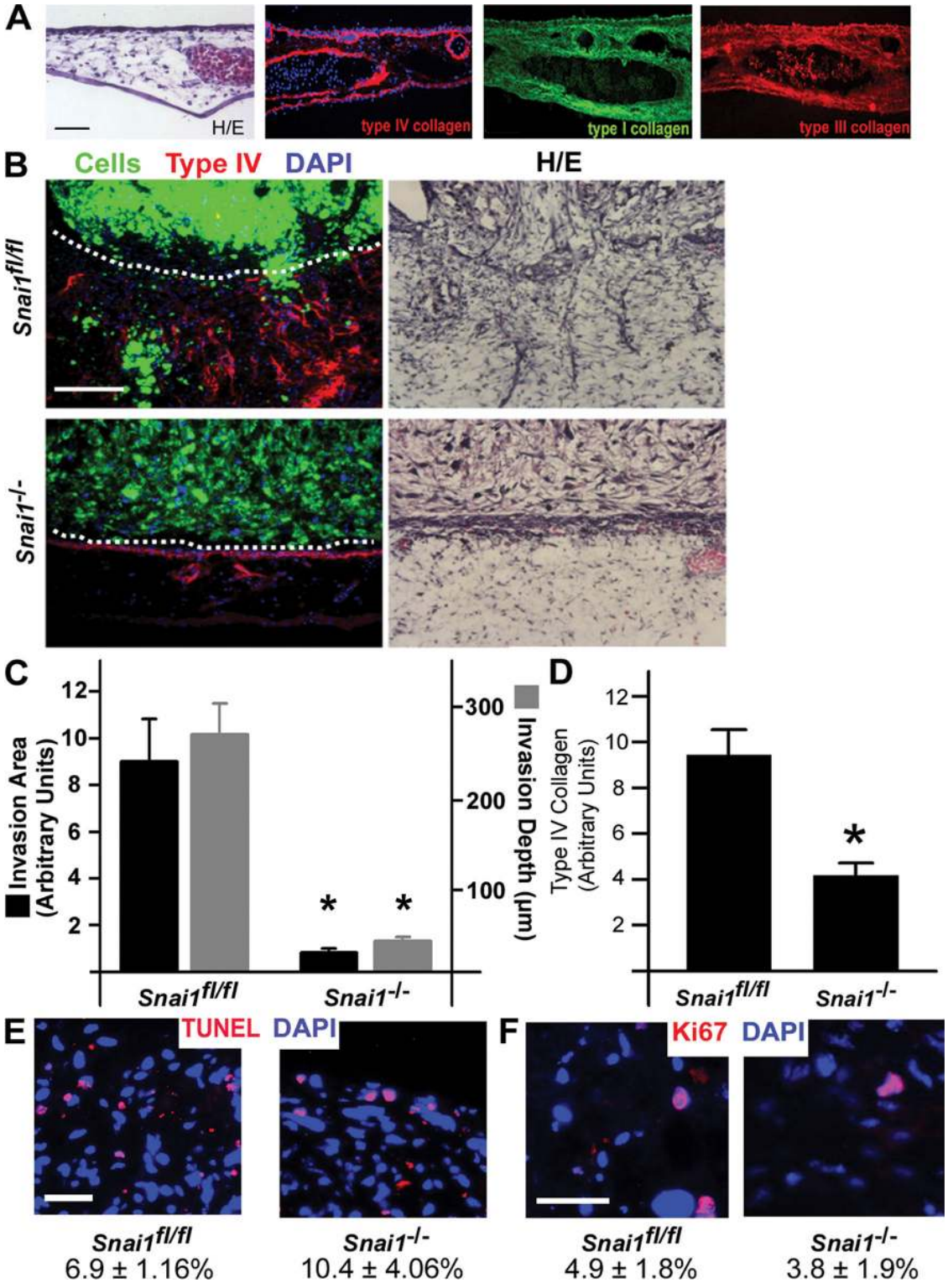

Figure 5. **Snail1 and the fibroblast wound response in vivo.** (A) CAM sections were stained with (left to right) hematoxylin and eosin (H/E) or antibodies against type IV, I, and III collagens, and photographed using light or fluorescence microscopy. (B) *Snai1*$^{fl/fl}$ or *Snai1*$^{-/-}$ fibroblasts were labeled with green fluorescent nanobeads, and cultured atop the live CAM. After 24 h, CAMs were sectioned and assessed for invasion by fluorescence microscopy for labeled cells (green), type IV collagen (red), cell nuclei (left, blue), or H/E staining (right). The broken line marks the upper surface of the CAM. Bar, 100 μm. (C) CAM invasion was quantified by measuring the invasive area demarcated by distribution of fluorescent beads in the CAM stroma or the depth of the invasive front (n = 5; mean ± SEM). *, P = 0.02 for invasion area; *, P = 0.01 for invasion depth. (D) Using type IV collagen signal in the CAM interstitium as an index of neovessel formation, CAM stromal angiogenesis was quantified (n = 11 for wild-type, n = 9 for null; mean ± SEM, *P < 0.01). (E) CAM sections were stained for the apoptosis marker TUNEL (red) and counterstained with DAPI (blue), and the percentage of TUNEL-positive cells was quantified (n = 3; mean ± SEM). (F) CAM sections were stained for the proliferation marker Ki67 (red), nuclei were counterstained with DAPI (blue), and the percentage of Ki67-positive nuclei was quantified (n = 3; mean ± SEM). Bars: (A and B) 100 μm; (E and F) 50 μm.

conditions, GO analyses revealed that major shifts had occurred in fibroblast behavior in the absence of Snail1 expression, with changes concentrated in functional programs tightly linked to cell adhesion, migration, proteolysis, and morphogenesis. Among Snail1-regulated targets, cortactin has been found to regulate MT1-MMP–dependent proteolysis, an activity critical for mesenchymal cell trafficking through ECM barriers (Chun et al., 2004; Sabeh et al., 2004; Filippov et al., 2005; Artym et al., 2006; Hotary et al., 2006; Clark et al., 2007). As such, the defects in cortactin and MT1-MMP expression and function observed in Snail1-deficient fibroblasts, in tandem with predicted changes in accessory molecules such as rhoA, ROCK, myosin light chain kinase, and tropomyosin, correlated with a marked loss in collagenolytic potential as well tissue-invasive activity in vitro and in vivo. Snail1-deleted fibroblasts were also unable to initiate an angiogenic response, a result likely consistent with the ability of MT1-MMP to induce angiogenesis by generating bioactive collagen fragments, regulating VEGF expression, or mediating semaphorin 4D shedding (Sounni et al., 2004; Weathington et al., 2006; Basile et al., 2007).

To date, analyses of Snail1 function in mammalian cells have focused on the ability of the transcription factor to initiate the transdifferentiation of normal or neoplastic epithelial cells. The findings presented herein, coupled with the fact that Snail1 protein is expressed in fibroblasts localized at damaged or carcinomatous tissues in vivo (Franci et al., 2006; Rosivatz et al., 2006), demonstrate that Snail1 activity is not confined to epithelial cells alone. Although our studies have focused on the role of Snail1 in regulating fibroblast function, it is intriguing to note that Snail1 may also be expressed in the neoplastic mesenchyme (Franci et al., 2006). Indeed, large T antigen/Ras-transformed fibroblasts are similarly reliant on Snail1 for the expression of a tissue-invasive phenotype (Fig. S3, available at http://www.jcb.org/cgi/content/full/jcb.200810113/DC1). Hence, in addition to its essential roles in EMT, we propose that Snail1 now be considered as a transcription factor capable of exerting key regulatory effects in the mesenchyme during development as well as disease.

Materials and methods

Mice

To generate the *Snai1* conditional knockout mouse, a targeting vector was constructed consisting of a flippase recognition target (FRT)-flanked phosphoglycerine kinase (PGK)-neo cassette 3′ to the loxp-flanked exon 3 of mouse *Snai1*, predicted to encode the two C-terminal zinc finger domains as well as the polyadenylation sequence for the *Snai1* mRNA. Approximately 4 kb of flanking genomic sequence was then inserted at the 5′ and 3′ ends of the loxp-flanked exon and FRT-flanked neomycin cassette to promote homologous recombination. The linearized targeting vector was electroporated into W4 embryonic stem cells (Auerbach et al., 2000), and stable transfected clones were selected with G418. Clones were screened for targeting of the *Snai1* by Southern blotting, and recombination was verified at both the 5′ and 3′ ends of the construct. Of 100 clones screened, 3 were identified with correct targeting and used for injection into C57BL/6NCrl × (C57BL/6J × DBA/2J)F1 blastocysts to produce chimeric mice. Out of three chimeric lines produced, two lines transmitted the targeted *Snai1* allele (*Snai1*^{tm1Stjw}) through the germ line. β-actin FLPe mice (stock No. 003800; Jackson ImmunoResearch Laboratories) were backcrossed to C57/6J mice to generate a congenic strain before mating with chimeras for excision of the FRT-flanked PGK-neo cassette to generate the *Snai1*^{fl} (*Snai1*^{tm2Stjw}) allele. *Snai1*$^{fl/fl}$ homozygous conditional knockout mice were born in the expected Mendelian ratios, which indicates that the *Snai1*^{fl} allele functions equivalently to the wild-type *Snai1* allele.

Antibodies and reagents

The 173EC2, 173EC3, and Sn9H2 anti-Snail1, and anti–MT1-MMP mAb1 antibodies were prepared and characterized as described previously (Franci et al., 2006; Rosivatz et al., 2006; Ingvarsen et al., 2008). The anti–GSK3-β phospho-serine 9 and anti-Akt phospho-serine 473 antibodies were obtained from Cell Signaling Technology. The anti-cortactin, anti-actin, and anti-Ki67 antibodies were obtained from Santa Cruz Biotechnology, Inc., Sigma-Aldrich, and Abcam, respectively. Adeno–β-gal and Adeno-Cre (transgenes driven by a cytomegalovirus promoter) were obtained from the University of Michigan Vector Core. LY-294002 and MG132 were obtained from EMD and Sigma-Aldrich, respectively. Apoptotic cell death was measured with an in situ apoptosis detection kit (ApopTag Red) according to the manufacturer's instructions (Millipore).

Western blotting

For Western blotting, the following primary antibody dilutions were used: 173EC2 hybridoma supernatant (1:40), 173EC3 affinity-purified antibody (1:10,000), anti–GSK3-β phospho-serine 9 and anti-Akt phospho-serine 473 antibodies (1:1,000), and anti-actin (1:4,000).

Quantitative PCR

Quantitative PCR was performed using the SYBR green PCR master mix (Applied Biosystems) according to the manufacturer's instructions. Primers for mouse cortactin were: forward, 5′-GCAGCCATCCCAGGTGTTTTAGTT-3′, and reverse, 5′-CTTTGGTCCCCTTTCCTCCTCTTC-3′; mouse MT1-MMP primers were: forward, 5′-TGATTCTGCCGAGCCCTGGACTGT-3′, and reverse, 5′-TGAGGGGGCATCTTTGTGGGTGAC-3′; mouse Snail primers were: forward, 5′-CTGCTTCGAGCCATAGAACTAAAG-3′, and reverse, 5′-GAGGGGAACTATTGCATAGTCTGT-3′; and glyceraldehyde 3-phosphate dehydrogenase primers were: forward, 5′-CCAAGGTCATCCATGACAACT-3′, and reverse, 5′-GTCATACCAGGAAATGAGCTTGACA-3′.

Immunofluorescence

For Snail1 immunocytochemistry, cells were fixed in 4% paraformaldehyde, permeabilized with 1% sodium dodecyl sulfate, denatured with 6M urea and 0.1% glycine, pH 3.5, blocked with 3% goat serum, and incubated with either 173EC2 (1:5) or 173EC3 (1:1,000) overnight, followed by detection with Alexa 488–labeled anti–mouse secondary antibody (Invitrogen). The Alexa 532–labeled anti–MT1-MMP mAb1 was used at 5 μg/ml, and the anti-cortactin antibody was used at a dilution of 1:40 after paraformaldehyde fixation and permeabilization with Triton X-100. The anti-cortactin antibody was detected with an Alexa 488–labeled, anti–rabbit secondary antibody (Invitrogen). Cells were counterstained with either 4′,6-diamidino-2-phenylindole or propidium iodide (Invitrogen). Confocal images of cells were acquired on a confocal microscope (FV500) using a 60× water immersion lens with a 1.20 numerical aperture using FluoView software (all from Olympus). All images comparing Snail1 wild-type and deficient cells were acquired with equal photomultiplier tube intensity and gain settings. Phase contrast images were acquired with a inverted microscope (DM-ILB; Leica) with a 20× objective and 0.40 numerical aperture, and CAM images were acquired on a microscope (DM-LB; Leica) with a 20× objective and 0.50 numerical aperture (Leica). Phase contrast and CAM images were acquired and analyzed with SPOT cameras and software (Diagnostic Instruments, Inc.).

Image analysis

To analyze MT1-MMP in invadopodia, confocal cross sections of invadopodia costained for MT1-MMP and cortactin were analyzed with MetaMorph software (MDS Analytical Technology). Collagen degradation was analyzed using ImageQuant 5.2 software (GE Healthcare). Invadopodial clusters were traced, and the areas containing MT1-MMP and cortactin colocalization were quantified.

Cell culture and invasion assays

To analyze 3D invasion, 50,000 fibroblasts were embedded in 100 μl of type I collagen gel (2.2 mg/ml) isolated from rat tail (Sabeh et al., 2004). After gelling, the plug was embedded in a cell-free, 500 μl collagen gel (2.2 mg/ml) cultured within a 24-well plate. After allowing the surrounding collagen matrix to gel (1 h at 37°C), fibroblast invasion was stimulated with serum and 10 ng/ml PDGF-BB (Millipore). Invasion distance from the inner collagen plug into the outer collagen gel was quantified. CAM invasion assays were conducted using 11-d-old chick embryos where fibroblasts labeled with Fluoresbrite-carboxylated nanospheres (Polysciences,

Inc.) were cultured atop the CAM for 24 h. Invasion depth was defined as the leading front of at least three invading cells in 10 fields in frozen sections (Sabeh et al., 2004). The invasion area was defined as the area occupied by invading cells in at least 10 fields (Sabeh et al., 2004), whereas angiogenesis was quantified by type IV collagen staining (Bajou et al., 2001). Snail1 conditional knockout transformed fibroblasts were generated by isolating embryonic day 13.5 mouse embryonic fibroblasts followed by serial retroviral introduction of the polyoma large T and activated Ras oncogenes (Land et al., 1983).

Transcriptional profiling

Total RNA was isolated from fibroblast cultures in 3D collagen, then labeled and hybridized to mouse 430 2.0 cDNA microarrays (Affymetrix). Three replicates each of Snail1 wild-type and deficient cultures were analyzed by the University of Michigan Microarray Core. Differentially expressed probe sets were determined using a minimum fold change of 1.5 and a maximum p-value of 0.005. GO analysis was performed to identify biological processes transcriptionally regulated by Snail. GO coefficients were calculated as −log(p-value).

Online supplemental material

Fig. S1 shows analysis of fibroblast function under 2D culture conditions. Fig. S2 shows transcript analysis by quantitative PCR and rescue of the Snail1-deficient phenotype by reconstitution with Snail1. Fig. S3 characterizes and analyzes the tissue-invasive potential of wild-type and Snail1-deficient transformed mouse embryonic fibroblasts. Table S1 shows a list of genes differentially expressed between Snail1 wild-type and deficient fibroblasts. Online supplemental material is available at http://www.jcb.org/cgi/content/full/jcb.200810113/DC1.

This work was supported by the National Institutes of Health (grant CA116516 to S.J. Weiss) and funds from the Cancer Biology Training Program (grant T32-CA009676) and the Breast Cancer Research Foundation. We thank E. Hughes (Transgenics Core) for technical assistance and Steve Lentz of the Morphology and Image Analysis Core (DK20572 and DK34933) for valuable assistance with confocal microscopy.

Submitted: 17 October 2008
Accepted: 24 December 2008

References

Artym, V.V., Y. Zhang, F. Seillier-Moiseiwitsch, K.M. Yamada, and S.C. Mueller. 2006. Dynamic interactions of cortactin and membrane type 1 matrix metalloproteinase at invadopodia: defining the stages of invadopodia formation and function. *Cancer Res.* 66:3034–3043.

Auerbach, W., J.H. Dunmore, V. Fairchild-Huntress, Q. Fang, A.B. Auerbach, D. Huszar, and A.L. Joyner. 2000. Establishment and chimera analysis of 129/SvEv- and C57BL/6-derived mouse embryonic stem cell lines. *Biotechniques.* 29:1024–1028, 1030, 1032.

Bajou, K., V. Masson, R.D. Gerard, P.M. Schmitt, V. Albert, M. Praus, L.R. Lund, T.L. Frandsen, N. Brunner, K. Dano, et al. 2001. The plasminogen activator inhibitor PAI-1 controls in vivo tumor vascularization by interaction with proteases, not vitronectin. Implications for antiangiogenic strategies. *J. Cell Biol.* 152:777–784.

Barrallo-Gimeno, A., and M.A. Nieto. 2005. The Snail genes as inducers of cell movement and survival: implications in development and cancer. *Development.* 132:3151–3161.

Basile, J.R., K. Holmbeck, T.H. Bugge, and J.S. Gutkind. 2007. MT1-MMP controls tumor-induced angiogenesis through the release of semaphorin 4D. *J. Biol. Chem.* 282:6899–6905.

Batlle, E., E. Sancho, C. Franci, D. Dominguez, M. Monfar, J. Baulida, and A. Garcia De Herreros. 2000. The transcription factor snail is a repressor of E-cadherin gene expression in epithelial tumour cells. *Nat. Cell Biol.* 2:84–89.

Bhowmick, N.A., E.G. Neilson, and H.L. Moses. 2004. Stromal fibroblasts in cancer initiation and progression. *Nature.* 432:332–337.

Boutet, A., C.A. De Frutos, P.H. Maxwell, M.J. Mayol, J. Romero, and M.A. Nieto. 2006. Snail activation disrupts tissue homeostasis and induces fibrosis in the adult kidney. *EMBO J.* 25:5603–5613.

Cano, A., M.A. Perez-Moreno, I. Rodrigo, A. Locascio, M.J. Blanco, M.G. del Barrio, F. Portillo, and M.A. Nieto. 2000. The transcription factor snail controls epithelial-mesenchymal transitions by repressing E-cadherin expression. *Nat. Cell Biol.* 2:76–83.

Carver, E.A., R. Jiang, Y. Lan, K.F. Oram, and T. Gridley. 2001. The mouse snail gene encodes a key regulator of the epithelial-mesenchymal transition. *Mol. Cell. Biol.* 21:8184–8188.

Chun, T.H., F. Sabeh, I. Ota, H. Murphy, K.T. McDonagh, K. Holmbeck, H. Birkedal-Hansen, E.D. Allen, and S.J. Weiss. 2004. MT1-MMP-dependent neovessel formation within the confines of the three-dimensional extracellular matrix. *J. Cell Biol.* 167:757–767.

Clark, E.S., A.S. Whigham, W.G. Yarbrough, and A.M. Weaver. 2007. Cortactin is an essential regulator of matrix metalloproteinase secretion and extracellular matrix degradation in invadopodia. *Cancer Res.* 67:4227–4235.

Dong, J., J. Grunstein, M. Tejada, F. Peale, G. Frantz, W.C. Liang, W. Bai, L. Yu, J. Kowalski, X. Liang, et al. 2004. VEGF-null cells require PDGFR alpha signaling-mediated stromal fibroblast recruitment for tumorigenesis. *EMBO J.* 23:2800–2810.

Escriva, M., S. Peiro, N. Herranz, P. Villagrasa, N. Dave, B. Montserrat-Sentis, S.A. Murray, C. Franci, T. Gridley, I. Virtanen, and A. Garcia de Herreros. 2008. Repression of PTEN phosphatase by Snail1 transcriptional factor during gamma radiation-induced apoptosis. *Mol. Cell. Biol.* 28:1528–1540.

Filippov, S., G.C. Koenig, T.H. Chun, K.B. Hotary, I. Ota, T.H. Bugge, J.D. Roberts, W.P. Fay, H. Birkedal-Hansen, K. Holmbeck, et al. 2005. MT1-matrix metalloproteinase directs arterial wall invasion and neointima formation by vascular smooth muscle cells. *J. Exp. Med.* 202:663–671.

Franci, C., M. Takkunen, N. Dave, F. Alameda, S. Gomez, R. Rodriguez, M. Escriva, B. Montserrat-Sentis, T. Baro, M. Garrido, et al. 2006. Expression of Snail protein in tumor-stroma interface. *Oncogene.* 25:5134–5144.

Gao, Z., T. Sasaoka, T. Fujimori, T. Oya, Y. Ishii, H. Sabit, M. Kawaguchi, Y. Kurotaki, M. Naito, T. Wada, et al. 2005. Deletion of the PDGFR-beta gene affects key fibroblast functions important for wound healing. *J. Biol. Chem.* 280:9375–9389.

Gimona, M., R. Buccione, S.A. Courtneidge, and S. Linder. 2008. Assembly and biological role of podosomes and invadopodia. *Curr. Opin. Cell Biol.* 20:235–241.

Grinnell, F. 2003. Fibroblast biology in three-dimensional collagen matrices. *Trends Cell Biol.* 13:264–269.

Herranz, N., D. Pasini, V.M. Diaz, C. Franci, A. Gutierrez, N. Dave, M. Escriva, I. Hernandez-Munoz, L. Di Croce, K. Helin, et al. 2008. Polycomb complex 2 is required for E-cadherin repression by the Snail1 transcription factor. *Mol. Cell. Biol.* 28:4772–4781.

Hotary, K., X.Y. Li, E. Allen, S.L. Stevens, and S.J. Weiss. 2006. A cancer cell metalloprotease triad regulates the basement membrane transmigration program. *Genes Dev.* 20:2673–2686.

Hotary, K.B., E.D. Allen, P.C. Brooks, N.S. Datta, M.W. Long, and S.J. Weiss. 2003. Membrane type I matrix metalloproteinase usurps tumor growth control imposed by the three-dimensional extracellular matrix. *Cell.* 114:33–45.

Hou, Z., H. Peng, K. Ayyanathan, K.P. Yan, E.M. Langer, G.D. Longmore, and F.J. Rauscher III. 2008. The LIM protein AJUBA recruits protein arginine methyltransferase 5 to mediate SNAIL-dependent transcriptional repression. *Mol. Cell. Biol.* 28:3198–3207.

Ingvarsen, S., D.H. Madsen, T. Hillig, L.R. Lund, K. Holmbeck, N. Behrendt, and L.H. Engelholm. 2008. Dimerization of endogenous MT1-MMP is a regulatory step in the activation of the 72-kDa gelatinase MMP-2 on fibroblasts and fibrosarcoma cells. *Biol. Chem.* 389:943–953.

Iyer, V.R., M.B. Eisen, D.T. Ross, G. Schuler, T. Moore, J.C. Lee, J.M. Trent, L.M. Staudt, J. Hudson Jr., M.S. Boguski, et al. 1999. The transcriptional program in the response of human fibroblasts to serum. *Science.* 283:83–87.

Julien, S., I. Puig, E. Caretti, J. Bonaventure, L. Nelles, F. van Roy, C. Dargemont, A.G. de Herreros, A. Bellacosa, and L. Larue. 2007. Activation of NF-kappaB by Akt upregulates Snail expression and induces epithelium mesenchyme transition. *Oncogene.* 26:7445–7456.

Klapholz-Brown, Z., G.G. Walmsley, Y.M. Nusse, R. Nusse, and P.O. Brown. 2007. Transcriptional program induced by Wnt protein in human fibroblasts suggests mechanisms for cell cooperativity in defining tissue microenvironments. *PLoS ONE.* 2:e945.

Land, H., L.F. Parada, and R.A. Weinberg. 1983. Tumorigenic conversion of primary embryo fibroblasts requires at least two cooperating oncogenes. *Nature.* 304:596–602.

Li, X.Y., I. Ota, I. Yana, F. Sabeh, and S.J. Weiss. 2008. Molecular dissection of the structural machinery underlying the tissue-invasive activity of MT1-MMP. *Mol. Biol. Cell.* 19:3221–3233.

Martin, P. 1997. Wound healing–aiming for perfect skin regeneration. *Science.* 276:75–81.

Moreno-Bueno, G., E. Cubillo, D. Sarrio, H. Peinado, S.M. Rodriguez-Pinilla, S. Villa, V. Bolos, M. Jorda, A. Fabra, F. Portillo, et al. 2006. Genetic profiling of epithelial cells expressing E-cadherin repressors reveals a distinct role for Snail, Slug, and E47 factors in epithelial-mesenchymal transition. *Cancer Res.* 66:9543–9556.

Murray, S.A., K.F. Oram, and T. Gridley. 2007. Multiple functions of Snail family genes during palate development in mice. *Development.* 134:1789–1797.

Nieto, M.A. 2002. The snail superfamily of zinc-finger transcription factors. *Nat. Rev. Mol. Cell Biol.* 3:155–166.

Olmeda, D., M. Jorda, H. Peinado, A. Fabra, and A. Cano. 2007a. Snail silencing effectively suppresses tumour growth and invasiveness. *Oncogene.* 26:1862–1874.

Olmeda, D., G. Moreno-Bueno, J.M. Flores, A. Fabra, F. Portillo, and A. Cano. 2007b. SNAI1 is required for tumor growth and lymph node metastasis of human breast carcinoma MDA-MB-231 cells. *Cancer Res.* 67:11721–11731.

Olson, M.F., and E. Sahai. 2008. The actin cytoskeleton in cancer cell motility. *Clin. Exp. Metastasis.* In press.

Orimo, A., P.B. Gupta, D.C. Sgroi, F. Arenzana-Seisdedos, T. Delaunay, R. Naeem, V.J. Carey, A.L. Richardson, and R.A. Weinberg. 2005. Stromal fibroblasts present in invasive human breast carcinomas promote tumor growth and angiogenesis through elevated SDF-1/CXCL12 secretion. *Cell.* 121:335–348.

Peinado, H., D. Olmeda, and A. Cano. 2007. Snail, Zeb and bHLH factors in tumour progression: an alliance against the epithelial phenotype? *Nat. Rev. Cancer.* 7:415–428.

Rosivatz, E., K.F. Becker, E. Kremmer, C. Schott, K. Blechschmidt, H. Hofler, and M. Sarbia. 2006. Expression and nuclear localization of Snail, an E-cadherin repressor, in adenocarcinomas of the upper gastrointestinal tract. *Virchows Arch.* 448:277–287.

Sabeh, F., I. Ota, K. Holmbeck, H. Birkedal-Hansen, P. Soloway, M. Balbin, C. Lopez-Otin, S. Shapiro, M. Inada, S. Krane, et al. 2004. Tumor cell traffic through the extracellular matrix is controlled by the membrane-anchored collagenase MT1-MMP. *J. Cell Biol.* 167:769–781.

Sakurai-Yageta, M., C. Recchi, G. Le Dez, J.B. Sibarita, L. Daviet, J. Camonis, C. D'Souza-Schorey, and P. Chavrier. 2008. The interaction of IQGAP1 with the exocyst complex is required for tumor cell invasion downstream of Cdc42 and RhoA. *J. Cell Biol.* 181:985–998.

Sounni, N.E., C. Roghi, V. Chabottaux, M. Janssen, C. Munaut, E. Maquoi, B.G. Galvez, C. Gilles, F. Frankenne, G. Murphy, et al. 2004. Up-regulation of vascular endothelial growth factor-A by active membrane-type 1 matrix metalloproteinase through activation of Src-tyrosine kinases. *J. Biol. Chem.* 279:13564–13574.

Vega, S., A.V. Morales, O.H. Ocana, F. Valdes, I. Fabregat, and M.A. Nieto. 2004. Snail blocks the cell cycle and confers resistance to cell death. *Genes Dev.* 18:1131–1143.

Vernon, A.E., and C. LaBonne. 2006. Slug stability is dynamically regulated during neural crest development by the F-box protein Ppa. *Development.* 133:3359–3370.

Weathington, N.M., A.H. van Houwelingen, B.D. Noerager, P.L. Jackson, A.D. Kraneveld, F.S. Galin, G. Folkerts, F.P. Nijkamp, and J.E. Blalock. 2006. A novel peptide CXCR ligand derived from extracellular matrix degradation during airway inflammation. *Nat. Med.* 12:317–323.

Yamada, K.M., and E. Cukierman. 2007. Modeling tissue morphogenesis and cancer in 3D. *Cell.* 130:601–610.

Yamaguchi, H., and J. Condeelis. 2007. Regulation of the actin cytoskeleton in cancer cell migration and invasion. *Biochim. Biophys. Acta.* 1773:642–652.

Yook, J.I., X.Y. Li, I. Ota, E.R. Fearon, and S.J. Weiss. 2005. Wnt-dependent regulation of the E-cadherin repressor snail. *J. Biol. Chem.* 280:11740–11748.

Yook, J.I., X.Y. Li, I. Ota, C. Hu, H.S. Kim, N.H. Kim, S.Y. Cha, J.K. Ryu, Y.J. Choi, J. Kim, et al. 2006. A Wnt-Axin2-GSK3beta cascade regulates Snail1 activity in breast cancer cells. *Nat. Cell Biol.* 8:1398–1406.

Zhou, B.P., J. Deng, W. Xia, J. Xu, Y.M. Li, M. Gunduz, and M.C. Hung. 2004. Dual regulation of Snail by GSK-3beta-mediated phosphorylation in control of epithelial-mesenchymal transition. *Nat. Cell Biol.* 6:931–940.

Zhou, X., R.G. Rowe, N. Hiraoka, J.P. George, D. Wirtz, D.F. Mosher, I. Virtanen, M.A. Chernousov, and S.J. Weiss. 2008. Fibronectin fibrillogenesis regulates three-dimensional neovessel formation. *Genes Dev.* 22:1231–1243.